Materials Selection for High Temperature (750°-1000°C) Metallic Recuperators for Improved Efficiency Microturbines

Bruce A. Pint, Robert W. Swindeman, Karren L. More and Peter F. Tortorelli
Oak Ridge National Laboratory
Metals and Ceramics Division
Oak Ridge, Tennessee 37831-6156
Phone: (865) 576-2897, E-mail: pintba@ornl.gov

ABSTRACT

The incorporation of a primary surface recuperator is one method for significantly improving the energy efficiency of a microturbine. The goal of this work is to employ laboratory testing of foil material (≈75-125μm or 3-5mil thickness) to select alloys for higher temperature (750°-1000°C, 1400-1800°F) recuperator performance based on creep strength and corrosion resistance. Alloys of interest are high-Cr, Ni-base superalloys such as alloy 625 and aluminum-containing alloys such as Haynes alloy 214 and Plansee alloy PM2000, which is an oxide-dispersed FeCrAl. The interest in the latter two alloys is based on their corrosion resistance. Particularly in exhaust gas environments, chromia surface oxides are not sufficiently protective at high temperatures to achieve desired lifetimes. The formation of a slow-growing external alumina scale confers exceptional corrosion resistance for this application.

INTRODUCTION

In order to improve the efficiency of small (25-200kW) gas turbine engines (microturbines), one common strategy is to employ a recuperator to use exhaust gas to preheat in-coming air to the combustor[1,2] One of the most efficient and compact types of recuperators is a primary surface recuperator which uses thin-walled, corrugated cells to facilitate heat transfer. Primary surface recuperator technology is well-established, but is currently limited in temperature to approximately 600-650°C (1100-1200°F) due to the use of stainless steels[3]. This application requires both high strength, to resist creep at temperature, and corrosion resistance, particularly for the exhaust gas which contains water vapor (as a combustion product). Water vapor is known to accelerate the oxidation rate of chromia-forming steels [4-7]

Current recuperated microturbine efficiencies are less than 30% and one focus of the Department of Energy's Microturbines Program is to improve their efficiency[8]. There are several methods for improving efficiency including increasing the turbine rotor inlet temperature and/or pressure ratios. Increasing turbine temperatures also could increase the recuperator temperature which would significantly reduce the recuperator durability unless new materials were employed. High temperature alloys could increase the recuperator operating temperature and some recuperator designs using ceramics could function at even higher temperatures.[9] However, the maximum temperature for a primary surface recuperator (using thin metal walls) has not been determined.

The goal of this work is to employ laboratory testing of foil material (≈75-125μm or 3-5mil thickness) to select alloys for higher temperature (750°-1000°C, 1400-1800°F) recuperator performance. For this study, materials selection was primarily based on high temperature creep strength and corrosion resistance but ultimately fabricability and weldability must also be considered. There is little published data on alloy behavior in 5-10% water vapor environments and bulk metallic properties are not reliable indicators of performance of thin section components. Rather than mathematical modeling, this program is conducting "experimental modeling"--attempting to gauge performance of new materials without going to the expense of building recuperators out of each material. Ultimately, a maximum possible operating temperature for each alloy will be determined based on creep and corrosion data such that, for example, a 25,000h (3yr) recuperator lifetime could be anticipated.

Both Ni- and Fe-base alloys are being considered including Ni base alloys Haynes 214 and Alloy 625, and an oxide-dispersion strengthened FeCrAl, Plansee alloy PM2000. Because of higher Ni and Cr contents and processing to add an oxide dispersion, these alloys are significantly more expensive than austenitic stainless steels such as type 321, Table I. The objective of this study is to provide relevant performance data so that cost-benefit analyses can be conducted. This paper contains current data for these three alloys. Additional creep data and characterization will be required to confidently identify maximum operating temperatures for each material.

EXPERIMENTAL PROCEDURE

Four alloys were selected for initial characterization: two chromia-forming alloys: (1) type 321 stainless steel (Fe-17wt%Cr-

Table I. Estimated relative costs for the alloys in this program using type 321 stainless steel as a baseline.

Alloy	Relative Cost
Type 321	1
Alloy 625	5
Haynes 214	7
Plansee PM2000	10

11Ni-0.3Ti) and (2) Inconel 625 (Ni-21Cr-9Mo-4Fe-4Nb); and two alumina- forming alloys: (3) Haynes alloy 214 (Ni-16Cr-4Al-3Fe) and (4) PM2000 (Fe-19Cr-5Al-0.4Ti-0.5Y_2O_3) an oxide dispersion strengthened (ODS) FeCrAl alloy. Alloy 321 provides a baseline for current stainless steel performance in recuperators.

All of the testing was performed on foil specimens, typically 100μm (4 mil) thick. Bulk material was reduced to foil by a combination of hot and cold rolling and annealing at Oak Ridge National Laboratory. The exception was PM2000 which was provided by Plansee in foils of 50, 75 and 125μm thick.

Mechanical test specimens were laser cut from foils. The creep specimen was 114mm (4.5in.) long with a reduced section 25.4mm (1in.) long and 0.635mm (0.25in) wide. The shoulders were approximately 16mm wide. Pads of the same thickness as the foil were spot-welded on the shoulders for re-enforcement and 0.317mm (0.125in.) diameter pin holes were cut in the shoulders for gripping. Four tabs, cut from 100μm thick alloy 625 foil, were spot welded on the specimen shoulders near the 6.35mm radius filets that led from the shoulders to the reduced section. The tabs extended outward from the specimen shoulders a distance of 2-3mm. Extensometer heads were lightly clamped to the specimen shoulders and rested on the tabs to prevent slipping. The extensometer was rod-in-tube type that transmitted extension out of the hot zone of the furnace to averaging LVDT sensors. For tests at 850°C and below, Type K thermocouples were wired to the reduced section of the specimen at two locations. For temperatures above 850°C, Type S thermocouples were used. Because of the small section areas, specimens were dead loaded. Only a few kilograms were required to achieve stresses in the range of 70-200MPa Creep extension data were collected by a data acquisition system, converted to strain-time pairs, and plotted as creep curves.

The oxidation testing was performed in tube furnaces. For testing in air, the alumina furnace tubes were not sealed and the specimens were sometimes placed into annealed alumina crucibles with lids to collect any spalled oxide. For testing in air plus 10% (by volume) water vapor, the foil specimens were placed in annealed alumina racks to hold the specimens upright and allow the humid air to flow among the specimens. The ends of the alumina tube were sealed and the water vapor was controlled by a water injection system described elsewhere [7]. Specimens were approximately 2.5cm x 1.5cm and were cleaned in acetone and alcohol prior to exposure. The as-rolled surface finish was tested, with no additional surface preparation. Because of the relatively low temperatures (700°-900°C) cycles were either 100h or 500h. Specimens were weighed between cycles using a Mettler model AG245 balance.

After exposure, specimens were characterized by scanning electron microscopy and mounted in epoxy and polished metallographically in order to observe the oxide scale cross-section. Limited exposures were made at higher temperatures (1000°-1100°C) on 1mm thick specimens to quickly grow slightly thicker oxides that were suitable for transmission electron microscopy (TEM) characterization including microchemical analysis using energy dispersive x-ray (EDX)analysis. TEM specimens were made using focused ion beam (FIB)thinning[10]. The reason for including the 1mm thick specimens was that TEM cross-sections are extremely difficult to make on foil specimens. When foils were sectioned, there was very little material remaining. Thus, some characterization work was performed on thick specimens in order to better understand the oxide being formed on the alumina-forming foils.

RESULTS

Mechanical Properties

While these alloys may be expensive (Table I), they definitely provide a significant improvement over currently used alloys. Figure 1 compares the creep performance of foils of alloy 625, alloy 214 and PM2000 at 750°C with a load of 100MPa to a coarse-grained bar of austenitic stainless steel (Nippon alloy NF709 with 20%Cr) at 760°C/103MPa. All of the foils exhibited lower strains than the bar material, with PM2000 showing virtually no change with time.

The excellent performance of PM2000 also was observed at higher temperatures. Figure 2 shows creep data for several materials at 871-875°C with a load of 100MPa. Data for 125μm (5mil) PM2000 were compared to bulk alloys such as a Ta-modified 310 stainless steel, alloy 556 (Fe-20%Ni-18Co-22Cr-3Mo-2.5W-0.6Ta-1Mn-0.4Si-0.2Al) and a nickel aluminide alloy known for its good creep strength. After an initial transient period, the PM2000 foil showed very little additional elongation during more than 1300h of testing.

Figure 3 compares the creep rupture life of the three alloy foils at 100MPa as a function of temperature. Alloy 214 showed somewhat longer life than alloy 625 at each temperature. Both foils were 100μm thick but the average grain size on Haynes 214 was larger (≈40μm) than that of alloy 625 (≈10μm) which may explain the better creep resistance of alloy 214. In contrast, 125μm-thick PM2000 showed significantly better behavior at higher temperatures. Typical of dispersion strengthened alloys, PM2000 is extremely coarse

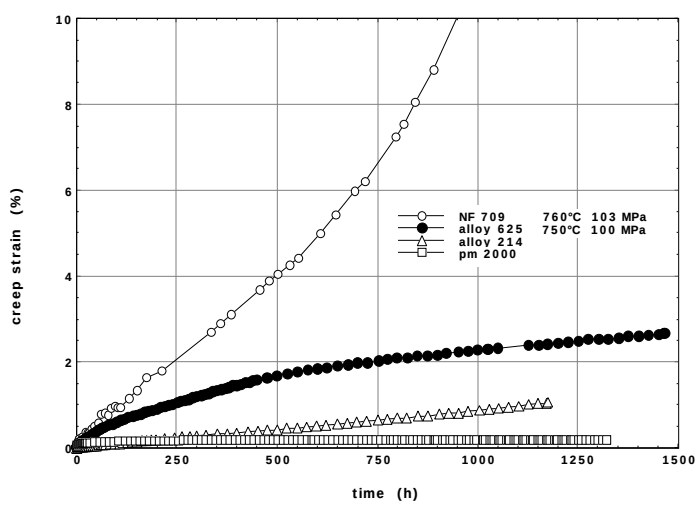

Figure 1. Comparison of creep curves for foil specimens tested at 750°C and 100MPa with a coarse-grained bar specimen of austenitic stainless steel (20%Cr) specimen tested at 760°C and 103MPa.

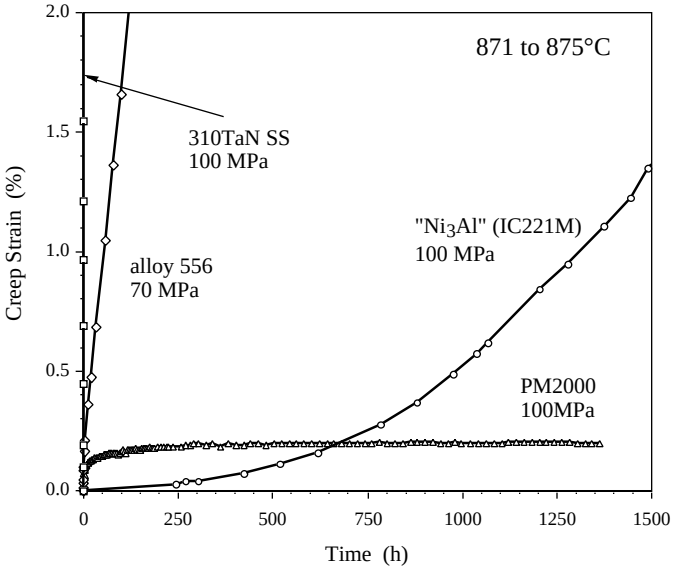

Figure 2. Comparison of the creep curve for PM2000 5mil foil specimen tested at 875°C with a load of 100MPa to data for bar materials, Ta-modified 310, alloy 556 and IC221M, a Ni_3Al-type alloy.

grained,with a grain size sometimes exceeding the foil thickness.

The next step will be to determine the effect of stress on each of these alloys in order to predict their behavior. Significantly lower stresses are expected in the recuperator. In order to specify the creep limited performance temperature for each alloy, the data set must be sufficient to predict behavior for various designs and stress levels specified by microturbine manufacturers.

Corrosion Resistance

For this application, the main area of interest is the effect of water vapor on the oxidation performance. These alloys are generally considered very corrosion resistant. However, because of the thin cross-section there is very little metal reservoir to maintain corrosion resistance for extended time periods (≈25,000h). Any increase in the oxidation rate could be catastrophic. Also, because creep is an equal concern, a significant loss in cross-section due to environmental attack could cause premature failure of the component by creep. Therefore, long term data (≥1000h) is being collected at 700-900°C in order to assess the oxidation performance of the various candidate alloys. Current results for the four foil materials are presented.

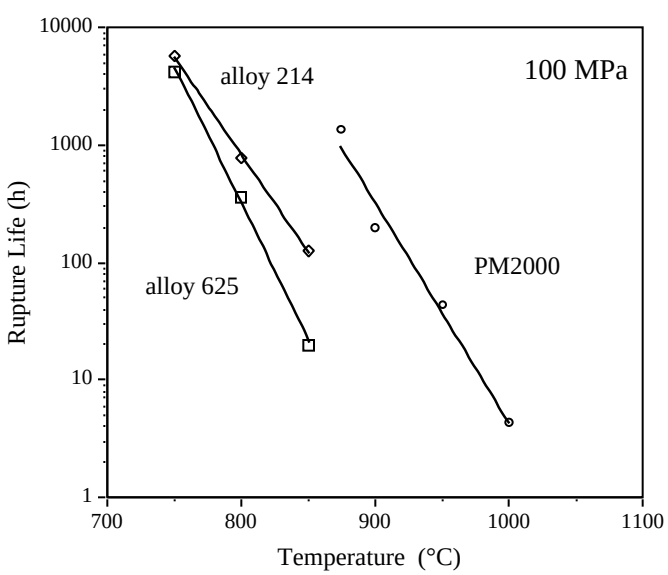

Figure 3. Creep rupture life at 100MPa for 100μm thick foil of Haynes 214 and Alloy 625 and for 125μm thick PM2000 foil.

The performance of type 321 stainless steel illustrates the concern about the effect of water vapor, Figure 4. For oxidation in air at 800°C, only low mass gains and very little scale spallation was observed. Based on the nominal 17%Cr level, this alloy is expected to show good oxidation resistance at this temperature and at lower temperatures. However, when water vapor was added to the environment, significant mass gains were noted for the foil material at 700° and 800°C. The mass gain data can be converted to oxide thickness by, multiply the mass gain (in mg/cm^2) by ≈6 to get oxide thickness (in μm). Thus, the addition of water vapor accelerated the rate of attack such that a significant fraction of the type 321 cross-section was consumed.

In contrast, alloy 625 showed much lower mass changes during the same exposure; note the difference in y-axis between Figures 4 and 5. Most notably, the addition of water vapor at 800°C did not increase the mass gain as it did for alloy 321. The slight mass losses at longer times at 800°C were likely due to loss by evaporation of CrO_3, which is increased by the presence of water vapor[4-7]. The improved performance of alloy 625 compared to alloy 321 is likely due to the higher Cr content (nominally 21.5%) in alloy 625. A similar beneficial effect of higher Cr contents has been observed previously[7]. The alloy 625 specimen exposed to air at 800°C showed a sharp mass increase at ≈1200h, but no additional increase was observed. At 900°C in air plus water vapor, the high mass gain followed by rapid mass loss indicates that the material does not have sufficient oxidation resistance to be used

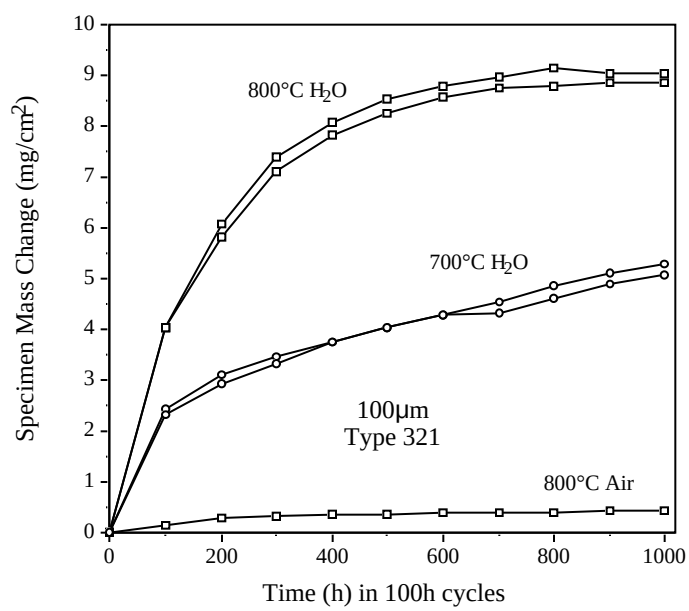

Figure 4. Oxidation data for 100μm (4mil) thick, type 321 stainless steel foil at 700° and 800°C with and without 10vol% H_2O. While this alloy is very oxidation resistant in air at 800°C, the addition of water vapor significantly increases the rate of attack at both 700° and 800°C. Two foil specimens were tested in the tests containing water vapor.

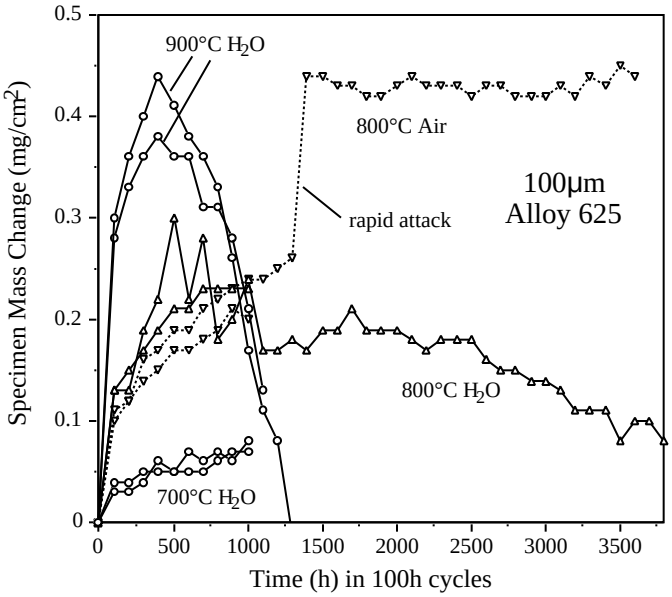

Figure 5. Oxidation data for 100µm (4mil) thick alloy 625 foil at 700°C-900°C in 100h cycles. At 700°C, the mass gain was very low, while at 900°C, high mass gains were quickly followed by mass losses. At 800°C, a sharp increase in mass gain was observed after 1200h in air, but no similar increase was observed in 10% water vapor, where the slight mass loss was likely due to evaporation of CrO_3.

at this temperature. Because of the low mass gains for alloy 625 at 700°C, this test was stopped at 1000h. In general, alloy 625 appears to be sufficiently oxidation resistant to be used in the 700-800°C temperature range.

In order to have sufficient oxidation performance at temperatures above 800°C, it will likely be necessary to switch to alumina-forming alloys. The growth rate of α-Al_2O_3 scales is significantly slower than Cr_2O_3 scales and alumina does not have a volatility problem like Cr_2O_3. Oxidation data at 900°C are shown in Figure 6 for several chromia- and alumina-forming alloy foils. While the 100µm chromia-forming foils (stainless steel with 20%Cr and Sandvik alloy 253MA) were rapidly attacked after a few thousand hours, the 50µm alumina-forming foils (Haynes 214, PM2000 and FeCrAl) have lifetimes of at least 10,000-20,000h. (None of these foils have failed at this time.) By switching to alumina-forming compositions (containing at least 4-5%Al), significantly better corrosion performance can be expected compared to stainless steels. However, like chromia-formers, the long-term effect of water vapor on the oxidation behavior remains a possible problem.

As an example of the improved performance of an alumina-forming alloy, Figure 7 shows data collected for Haynes 214 at 800-900°C. At 800°C, the addition of water vapor showed little effect and low mass gains were observed, with no mass losses like those observed for alloy 625 (Figure 5). At 900°C, the mass gain for 100µm thick foil in 100h cycles in air + 10%H_2O is compared to data for 50µm foil in 500h cycles in air. The initial mass gain was higher in water vapor but the steady state rate was not significantly different.

Figure 8 shows results at 700°-900°C for 125µm thick PM2000 foil, the same material being tested in creep, Figures 1-3. The mass gains increased with temperature as expected. The addition of water vapor at 800°C actually lowered the mass gain, indicating little effect

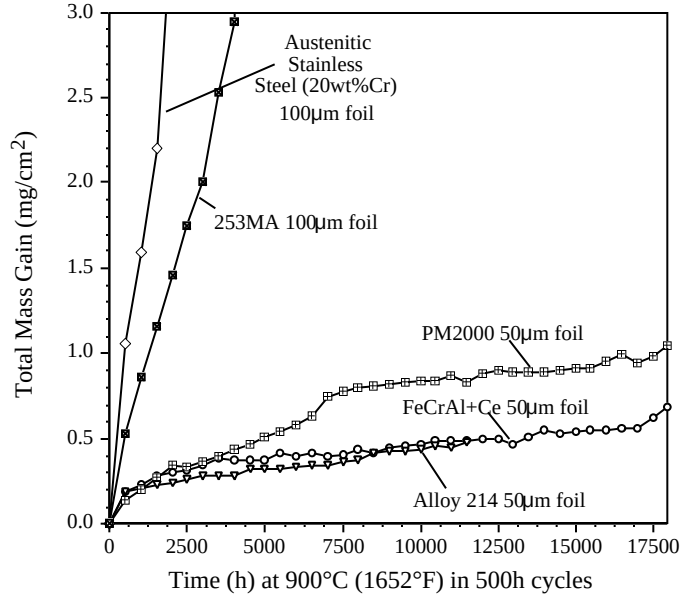

Figure 6. Mass gain data for various metal foils oxidized in 500h cycles at 900°C in air. Alloys which form chromia scales, such as stainless steels, undergo rapid mass gains while alloys which form alumina scales (MCrAl-type)show limited attack even at long times.

of the addition of water vapor. At 900°C, the initial mass gain was somewhat higher than for Haynes 214. With 1 mg/cm^2 equivalent to ≈5.4µm of Al_2O_3, a substantial oxide thickness (compared to the foil thickness) was formed in only a few hundred hours at 900°C. The subsequent steady-state rate was relatively low but a large loss in cross-sectional thickness (due to Al consumption) cannot be tolerated in this application. Previous work by Moseley et al.[11] indicated that water

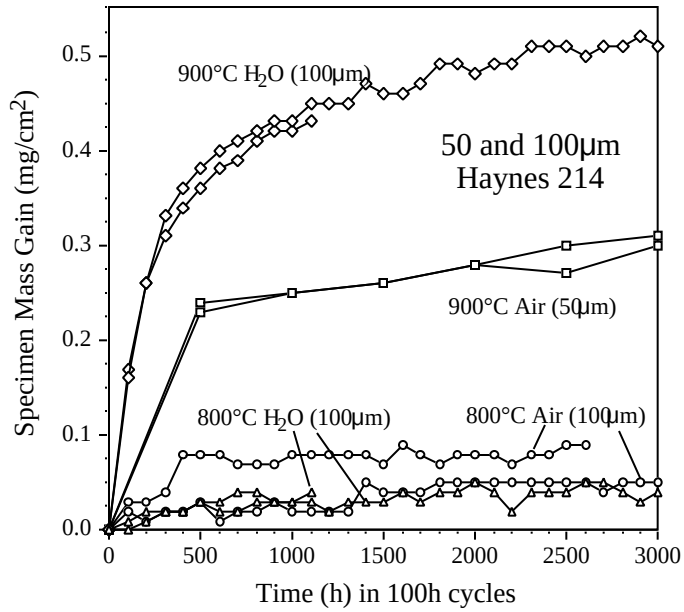

Figure 7. Oxidation data for 50 and 100µm (2 and 4 mil) thick, alloy 214 foil at 800° and 900°C with and without 10vol% H_2O. The addition of water vapor did not appear to affect the oxidation behavior at 800°C. Two foil specimens were tested in each condition.

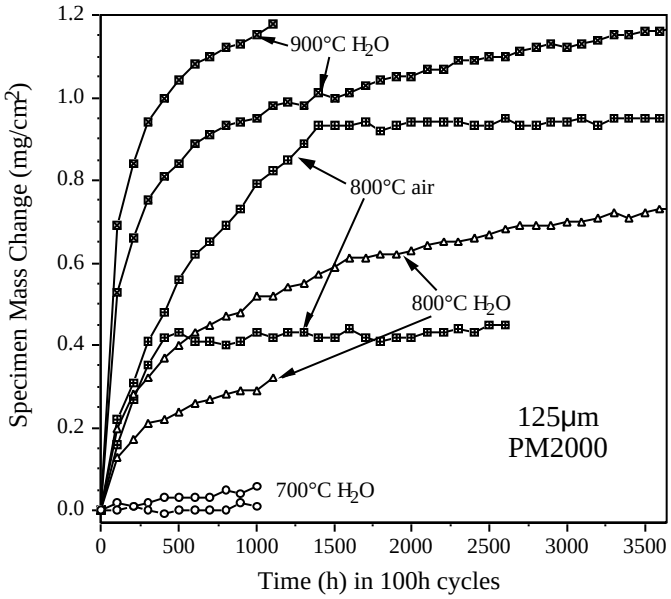

Figure 8. Oxidation data for 125μm (5mil) thick PM2000 (ODS FeCrAl) at 700°-900°C with and without 10vol% H_2O. The mass gains increase with temperature as expected. The addition of water vapor at 800°C actually lowered the mass gains.

vapor can stabilize the formation of metastable θ-Al_2O_3 on FeCrAlY which grows at a faster rate than α-Al_2O_3[12]. If exposure to water vapor has stabilized the metastable θ formation for a longer time period then this may explain the higher mass gains. One way to avoid the formation of θ-Al_2O_3 is to pre-oxidize PM2000 at a higher temperature or in a dry environment where α-Al_2O_3 forms. Once the stable α phase forms, slower mass gains would be expected. Haynes 214 may be less susceptible to the formation of θ-Al_2O_3 because it forms a transient Ni-rich scale (NiO or $NiAl_2O_4$) which may facilitate the formation of α-Al_2O_3. Further testing will be required to study the long-term oxidation performance of PM2000 at ≈900°C. Again, while its oxidation resistance may generally be excellent, in this application with a small cross-section, a transient effect could cause premature failure of the recuperator.

Characterization of Corrosion Products

One of the main goals of the characterization work was to obtain a better understanding of the water vapor effect on protective oxide formation. In order to produce specimens for characterization, short-time, high temperature (1000°-1100°C)experiments were conducted on foil and on 1mm thick specimens in a microbalance which provides continuous mass change data. A higher temperature was used because the scale is extremely thin at lower temperatures. These specimens are being evaluated while waiting for completion of some of the long-term oxidation testing at lower temperatures.

Haynes 214 was exposed for 100h at 1100°C with and without 10%H_2O. Similar to the results at 900°C (Figure 7), the addition of water vapor did not significantly change the mass gain at 1100°C, however, a slightly higher transient mass gain was noted. Figure 9 compares the metallographic cross-sections of the scale formed on 1mm thick material using light microscopy. The oxides appear similar in thickness although the metal-scale interface appears slightly rougher

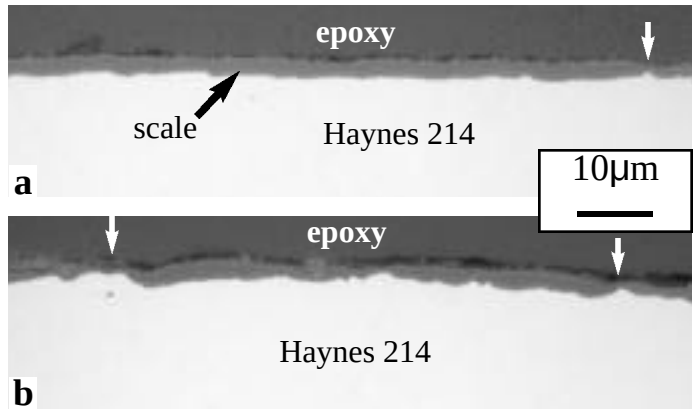

Figure 9. Metallographic cross-sections of the scale formed on Haynes 214 after 100h at 1100°C in (a) air and (b) air plus 10% water vapor. With the addition of water vapor (b), the metal-oxide interface appeared rougher and the oxide appeared less uniform in thickness.

with the addition of water vapor. In both cases, there appear to be areas where the scale has spalled, leaving locally thinner oxide (arrows). At this magnification, it is difficult to differentiate the Ni-rich outer scale from the inner alumina scale, thus it cannot be determined if the outer layer has spalled. These cross-sections will be further examined using SEM.

Portions of these same specimens were sectioned for TEM analysis. An example of the cross-section formed in 10%H_2O is shown in Figure 10. In both cases, the scale consisted of an outer Ni-rich oxide ($NiAl_2O_4$) with an inner α-Al_2O_3 layer. This outer $NiAl_2O_4$ layer is typical on Ni-base alloys without sufficient Al to directly form Al_2O_3. The $NiAl_2O_4$ grain structure is relatively equiaxed while Al_2O_3

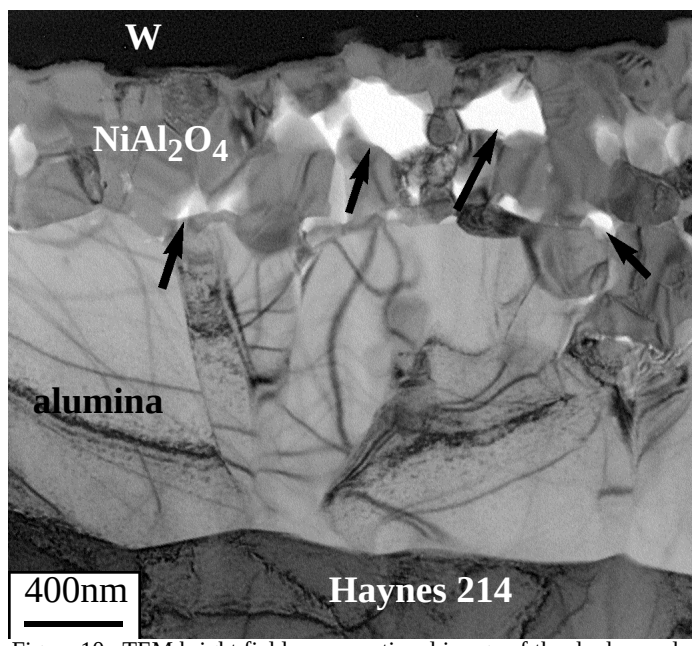

Figure 10. TEM bright field cross-sectional image of the duplex scale formed on Haynes 214 (NiCrAlFe+Y/Zr) after 100h at 1100°C in air + 10%H_2O. Compared to the oxide formed in air, this oxide was slightly thicker and contained more voids (arrow). During FIB specimen preparation, the outer surface is coated with a protective W layer.

has the columnar grain structure typically formed on alloys containing reactive elements[13]. In this case Y and Zr are added to Haynes 214 in order to slow the scale growth rate and improve the alumina scale adhesion.

The main effect of water vapor at this temperature appeared to be a slightly thicker total scale thickness particularly in the transient Ni-rich oxide. This observation is supported by the mass changes (e.g. Figure 7). In the TEM cross-sections, it also appears that there are more voids in the scale formed in water vapor, particularly in the outer oxide and at the $NiAl_2O_4$-Al_2O_3 interface (arrows in Figure 10).

Using TEM/EDX analysis of the oxide grain boundaries, both Y and Zr ions were found segregated to the Al_2O_3 grain boundaries. Because of the low Y(20ppma) and Zr(120ppma) contents in this alloy, no Y- or Zr-rich precipitates were observed in either the alloy or the oxide. This type of segregation behavior has also been widely observed[13]

Specimens of PM2000 were oxidized at 1000°C for 100h with and without water vapor. Again the addition of water vapor did not substantially change the total mass gain at this temperature. Because of faster Cr and Al diffusion in ferritic alloys, PM2000 does not form any transient Fe-rich oxide. Figure 11 shows the oxides formed on PM2000. With the addition of water vapor, the alumina scale appeared rougher with apparent protrusions of oxide into the metal. These protrusions are not typical oxide "pegs" because there is no free Y in this alloy to internally oxidize[14]. Previous work on similar ODS alloys did not observe similar structures in air or O_2 environments[15]. Also, in some locations the oxide was thicker (Figure 11b) which may be the result of θ-Al_2O_3 formation as discussed earlier. However, in other areas, the scale appeared slightly thinner than that formed in air (Figure 11c). TEM specimens of these oxides are not yet complete. Of particular interest will be (1) the grain structure near the oxide protrusions which may reveal the cause of these structures and (2) the defect density with and without water vapor.

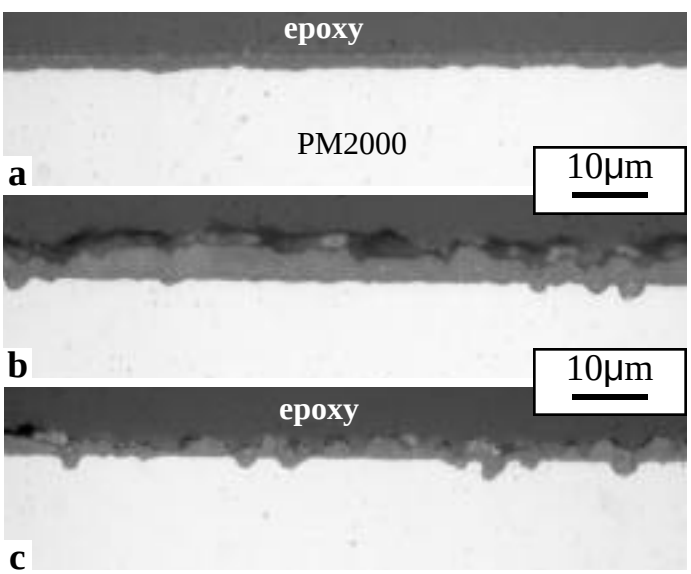

Figure 11. Metallographic cross-sections of the scale formed on PM2000 after 100h at 1100°C in air, (a), and air plus 10% water vapor (b) and (c). With the addition of water vapor, the metal-oxide interface appeared rougher with apparent oxide protrusions, in some areas (b) the scale appeared thicker than others (c).

DISCUSSION

These results represent work in progress to develop the data set needed to predict the performance of these alloys in a high temperature recuperator. In order to predict maximum operating temperatures for these alloys, microturbine manufacturers will need to specify parameters such as the component stress level and the acceptable amount of deformation as well as the desired lifetime.

At this time insufficient data have been collected to make these types of predictions. One important issue that has not been determined is the effect of stress on the creep rupture life. There are several concerns in this area. One is that, at lower stress levels, diffusion (or vacancy) creep may occur in the relatively fine grained Ni-base foil materials (625 and 214). Compared to power law creep where dislocation movement mechanisms may be controlling, diffusion creep is characterized by creep rates proportional to the stress level. This would severely reduce the lifetime of the foil material. Another area of concern for PM2000 is that abrupt failures were observed in many cases. Little deformation was observed for an extended period and then rapid failure. This type of behavior is very difficult to model with confidence.

Regarding the corrosion-limited performance temperature, some temperature limitations are apparent but longer-term testing is necessary to verify and refines these estimates. One of the reasons that the water vapor effect is being carefully studied is that there are no mechanistic models that have been proved to explain this effect. Therefore it is not known when an effect of water vapor may appear.

For the chromia-forming alloy 625, it appears clear that it will be limited to operation at ≤800°C. One remaining concern is that at longer times, as the alloy becomes depleted in Cr, accelerated attack may occur that could severely limit its predicted lifetime.

Similar uncertainties exist for Haynes 214 and PM2000. Currently it appears that both alloys could be operated for extended periods at 900°C. However, the lower strength of Haynes 214 could limit its use to lower temperatures, depending on the stress level in the recuperator. For PM2000, one area of concern is the high transient mass gains. However, there are possible strategies (discussed above) for limiting such problems.

In general, oxidation-limited lifetime predictions for this application are somewhat different than those examined in the literature, e.g. Ref. [16]. In those cases, lifetime is defined as the time to the formation of base-metal oxides (i.e. breakaway oxidation) when the Al or Cr content is sufficiently depleted. For this application, creep-related failure likely would occur long before breakaway oxidation due to loss of load-bearing cross-section. Thus, a new type of model with different failure criteria must be developed for this application.

A final area that has not been considered yet is the combined effect of oxidation and stress. An applied tensile stress may cause periodic cracking of the scale leading to localized accelerated attack and loss of cross-section that may lead to early creep failure. Current creep testing is being conducted in air but some future testing may be performed in a water vapor environment in order to consider this aspect.

SUMMARY

The goal of this work is to determine the maximum temperature at which a primary surface recuperator could be operated and still achieve an extended life. Creep and corrosion data have been collected for three candidate alloys, alloy 625, Haynes 214 and Plansee PM2000, being considered for this application. Creep rupture testing has been

performed as a function of temperature at 100MPa. Corrosion testing has been conducted for up to 4000h at 700°-900°C in air with 10%H_2O. More data collection and characterization work is necessary to complete these maximum temperature predictions for these alloys.

While these alloys currently may be considered too expensive for commercial microturbines, it appears that they can significantly increase the current maximum operating temperature of a primary surface recuperator. The recent increases in fuel prices has placed a renewed emphasis on efficiency that may result in advanced alloys being considered in the future because of their performance benefits including higher temperatures and/or greater durability.

ACKNOWLEDGMENTS

The authors would like to thank M. Howell, G. Garner and S. Trent at ORNL for assistance with the experimental work and I. G. Wright and J. A. Haynes at ORNL for their comments on the manuscript. This research was sponsored by the U.S. Department of Energy, Office of Power Generation Technology, Microturbines program under contract DE-AC05-00OR22725 with UT-Battelle, LLC.

REFERENCES

1. Watts, J. H., 1999, “Microturbines: A New Class of Gas Turbine Engine,” Global Gas Turbine News, **39**(1), pp.4-8.
2. Hamilton, S. L., 1999, “Microturbines Poised to Go Commercial,” Modern Power Systems, **19**(9), pp.21-22.
3. Ward, M. E., 1995, “Primary Surface Recuperator Durability and Applications,” Report No.TTS006/395, Solar Turbines, Inc., San Diego, CA.
4. Caplan, D. and Cohen, M., 1959, "High Temperature Oxidation of Chromium-Nickel Steels," Corrosion, **15**, pp.57-62.
5. W. J. Quadakkers and P. J. Ennis, 1998, "The Oxidation Behavior of Ferritic and Austenitic Steels in Simulated Power Plant Service Environments," Materials for Advanced Power Engineering 1998, J. Leconte-Beckers, F. Schubert and P. J. Ennis Eds, Forschungszentrum, Jülich Germany, pp.123-38.
6. H. Nickel, Y. Wouters, M. Thiele and W. J. Quadakkers, 1998, "The Effect of Water Vapor on the Oxidation Behavior of 9%Cr Steels in Simulated Combustion Gases,” Fresenius Journal of Analytical Chemistry, **361**, pp.540-4.
7. Pint, B. A. and Rakowski, J. M., 2000, “Effect of Water Vapor on the Oxidation Resistance of Stainless Steels,” NACE Paper 00-259, Houston, TX, presented at NACE Corrosion 2000, Orlando, FL, March 2000.
8. Energetics, Inc., 1999, “Summary of the Microturbine Technology Summit,” Report No. DOE/ORO 2081, Oak Ridge, TN.
9. Omatete, O., Maziasz, P. J., Pint, B. A. and Stinton, D. P., 2000, “Recuperators for Advanced Microturbines,” Report No.ORNL/TM-2000/304, Oak Ridge National Laboratory, Oak Ridge, TN.
10. K. L. More, D. W. Coffey, B. A. Pint, K. S. Trent and P. F. Tortorelli, “TEM Specimen Preparation of Oxidized Ni-Based Alloys Using the Focused Ion Beam (FIB) Technique,” (Paper presented at Microscopy and Microanalysis 2000, Philadelphia, PA, August 2000).
11. Moseley, P. T., Hyde, K. R., Bellamy, B. A. and Tappin, G., 1984, “The Microstructure of the Scale Formed During the High Temperature Oxidation of a FeCr Alloy Steel,” Corrosion Science, **24**, pp.547-65.
12. Rybicki, G. C. and Smialek, J. L., 1989, “Effect of the θ-α-Al_2O_3 Transformation on the Oxidation Behavior of β-NiAl+Zr,” Oxidation of Metals, **31**, pp.275-304.
13. Pint, B. A., 1996, ‘“Experimental Observations in Support of the Dynamic Segregation Theory to Explain the Reactive Element Effect,” Oxidation of Metals, **45**, pp.1-37.
14. Kuenzly, J. D., and Douglass, D. L., 1974, ‘The Oxidation Mechanism of Ni_3Al Containing Yttrium,” Oxidation of Metals, **8**, pp.139-178.
15. Pint, B. A., Garratt-Reed, A. J. and Hobbs, L. W., 1995, “The Reactive Element Effect in Commercial ODS FeCrAl Alloys," Materials at High Temperature **13**, pp.3-16.
16. Quadakkers, W. J. and Bongartz, K., 1994, “The Prediction of Breakaway Oxidation for Alumina Forming ODS Alloys using Oxidation Diagrams,” Materials and Corrosion, **45**, pp.232-41. "